J. Synchrotron Rad. (1998). **5**, 723–725

A unique high-performance wide-range (10–1500 eV) spherical grating monochromator beamline

P.-C. Tseng,* C.-C. Chen, T.-E. Dann, S.-C. Chung, C. T. Chen and K.-L. Tsang

Synchrotron Radiation Research Center, Hsinchu 300, Taiwan. E-mail: tpc@bl11b.srrc.gov.tw

(*Received 4 August 1997; accepted 26 September 1997*)

A wide-spectral-range high-performance 6 m-spherical grating monochromator (6 m-SGM) beamline has been designed and is under construction at SRRC. Two different entrance slits, instead of additional mirrors, are used to optimize the overall performance. Six gratings are used to cover photon energies from 10 to 1500 eV. Movable entrance slits and bendable vertical focusing mirrors are used to enhance further the beamline performance. A bendable horizontal focusing mirror is used to improve the resolution and to focus the photon beam at the experimental station immediately after the exit slit. Several end-stations can be installed at the same time to utilize the beam time fully. The expected energy-resolving power, with both slit openings set at 10 μm, is up to 15 000 and 40 000 for the high- and low-energy branches, respectively. A photon flux of 1×10^{11} photons s^{-1} can be obtained with an energy-resolving power of 20 000.

Keywords: spherical grating monochromator beamline; high-performance spherical grating monochromator; wide range.

1. Introduction

In the past ten years, the development of the VUV and soft X-ray beamlines, covering photon energies from 10 to 2000 eV, has gone through major advances. The newly developed beamlines have achieved their design goals of high resolution and high flux. Among various designs, SX-700 (Petersen, 1982; Jark, 1992; Domke *et al.*, 1992; Kanindl *et al.*, 1992) and Dragon (Chen, 1987; Chen & Sette, 1989; Warwick *et al.*, 1995; Schulz *et al.*, 1996) are the most commonly used. In addition to high resolution, SX-700 and other PGM-type designs have the advantage of covering a wide spectral range per grating. However, the ultra-high precision elliptical pre-focusing mirror needed for SX-700 to achieve high resolution is very difficult to obtain. New PGM-type designs such as those of Koike & Namioka (1994, 1995) utilize variable-spacing plane gratings and require an additional mirror with a sophisticated motion (a coupled translation and rotation) to comply with the grating rotation. This kind of design could degrade the energy resolution because of the figure error of the additional mirror and the complicated energy-scanning mechanism. On the other hand, the Dragon beamline uses only ultra-high-precision spherical (or cylindrical) optical components, which are relatively easy to manufacture. Moreover, only a simple grating rotation mechanism is needed for scanning the energy. In fact, thanks to its simplicity, a resolving power as high as 65 000 has recently been achieved by a Dragon-type SGM beamline (Schulz *et al.*, 1996). There are two Dragon-type beamlines, the 6 m-LSGM (Tseng *et al.*, 1995) and the 6 m-HSGM (Chung *et al.*, 1995) beamline, which have been operational at SRRC since 1994. These beamlines have an outstanding performance and offer user-friendly operation. However, there is still a strong demand for a high-performance beamline which can cover photon energies in the range 10–1500 eV. In order to fulfill the goal of obtaining a wide spectral range without sacrificing the high performance of the SGM design, we have come up with a design that utilizes two different entrance slits to achieve different grating included angles, instead of adding mirrors between the entrance and exit slits. In this design, there is only one reflection optics component, *i.e.* the grating, between the slits. Furthermore, we have added several special features to the original Dragon design to enhance the performance greatly.

2. Beamline optical system

The optical layout of the wide-range 6 m-SGM beamline is shown in Fig. 1 and the parameters of the optical components are listed in Table 1. Similar to other Dragon-type designs, a 6 m-SGM is arranged between pre-focusing and post-focusing mirrors. Two separate entrance slits are utilized to achieve two different grating included angles. We have also utilized several special features, such as a bendable modified plane–elliptical horizontal focusing mirror (HFM), bendable vertical focusing mirrors (VFM) and movable entrance slits, to enhance further the performance.

The HFM, which is located 5.5 m from the source, collects 11 mrad of the horizontal radiation fan from the source. Since this mirror will receive a thermal loading of 100 W, the HFM is internally water cooled. The HFM is a specially designed plane–ellipse. The shape of the ellipse is calculated directly from the geometric arrangement of the optical system and the actual arc

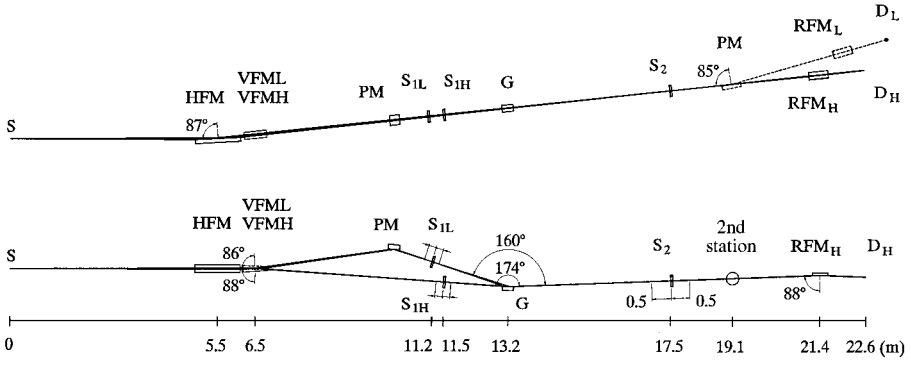

Figure 1
Optical layout of the wide-range 6 m-SGM beamline.

Table 1
Optical parameters of wide-range 6 m-SGM beamline.

Abbreviations used are as follows: horizontal pre-focusing mirror (HFM), vertical pre-focusing mirror (VFMH), vertical pre-focusing mirror (VFML), plane mirror (PM), grating (GH), grating (GL), refocusing mirror (RFM).

	HFM	VFMH	VFML	PM	GH	GL	RFM
r_1 (cm)	550	650	650		172	213	~400
r_2 (cm)	1200–1400	500	476.6		380–480	380–480	120
Deviation angle (°)	174	176	172	154	174	160	176
Type	Plane–ellipse (water-cooled)	Tangential cylinder	Tangential cylinder	Plane	Sphere	Sphere	Toroidal
Size ($L \times W \times H$) (cm^3)	120 × 7 × 9	55 × 10 × 5	55 × 10 × 5	10 × 10 × 5	18 × 5 × 3	18 × 5 × 3	60 × 10 × 5
Coating	Au	Au	Au	Au	Au	Au	Au
Substrate	Glidcop	Zerodur	Zerodur	Zerodur	Zerodur	Zerodur	Zerodur
Curvature (cm)	14000–16000	16195	7884	∞	5550	1780	R = 5290, r = 6.4
Ruling profile					Laminar mask 1:1	Laminar mask 1:1	
Ruling density (lines mm^{-1})					400 800 1600	300 600 1200	
Ruling depth (Å)					130 65 30	500 250 150	

shape of the bending-magnet source (Chen, 1997). The modified plane–elliptical surface can eliminate the aberration effect caused by the source, and hence provide a much better focused spot. The modified plane–ellipse is now commercially available. The HFM is made bendable so that the photon beam can be focused horizontally onto the exit slit or at the sample position. The horizontal size of the photon beam at the exit slit or at the sample position is about 1 mm. The experimental station immediately after the exit slit is very suitable for experiments that require high photon flux, especially in the high-energy region.

Two cylindrical VFMs, one for the low-energy branch and the other for the high-energy branch, are employed to provide two different optical paths. Both VFMs are bendable and their radii can be continuously varied, so that the photon beams can always be focused vertically onto the movable entrance slits. The entrance slits are made movable as this allows eliminatination of the coma aberration of the grating. The photon beam of the low-energy branch is focused vertically and deflected upwards by VFML and then reflected downwards by a plane mirror. This arrangement gives a smaller grating included angle and provides enough space to accommodate both entrance slits. With the help of the *SHADOW* ray-tracing programs (Lai & Cerrina, 1986), a demagnification factor of about 1.5 is decided upon for the VFM to minimize the focused spot size at the entrance slit.

Included angles of 174 and 160° are chosen for the high- and low-energy branches, respectively. Six spherical gratings are used to cover photon energies from 10 to 1500 eV. Gratings with ruling densities of 300, 600 and 1200 lines mm^{-1} are used to cover the low-energy branch from 10 to 150 eV, and gratings with ruling densities of 400, 800 and 1600 lines mm^{-1} are used to cover the high-energy branch from 130 to 1500 eV. A laminar ruling profile is used for each grating to reduce the amount of high-order scattered light. A common movable exit slit is used for the entire energy range. A single toroidal re-focusing mirror (RFM) is used to focus the beams onto the sample. One plane mirror and another RFM can be inserted later for the third experimental station. The final focused image at the last sample position is smaller than 0.7 × 0.3 mm.

3. Estimated performance

Following the Dragon beamline design criteria (Chen, 1987), the performance of the wide-range 6 m-SGM is optimized. Incident angles of 80 and 87° are chosen for the low- and high-energy ranges, respectively, and the sum of the entrance and exit arms of the monochromator is set at 6 m to maximize the energy resolution and photon throughput. In order to increase the resolution limits, spherical gratings are used to minimize the astigmatic coma term (C_{12}) and astigmatic term (C_{02}), and a movable exit slit is used to eliminate the defocus term (C_{20}). Spherical gratings rather than the cylindrical gratings are used here because spherical gratings are slightly easier to manufacture. If the entrance slit is kept fixed, the coma (C_{30}) aberration may limit the ultimate resolution of the momochromator. The energy-resolving power of the 6 m-SGM with a fixed entrance is shown by the dashed curves in Fig. 2. The resolving power of each grating has a maximum in the middle and falls off on both sides, due to the coma term. The energy-resolving power can be improved further by eliminating the C_{30} term. By moving both the entrance and exit slits to satisfy Rowland-circle focusing conditions (Samson, 1967), *i.e.* $r_1 = R\cos\alpha$ and $r_2 = R\cos\beta$, both the C_{20} and C_{30} terms can be eliminated at the same time. Fig. 2 displays the resolving powers under this condition, showing a maximum value of 40 000. In these calculations, the figure slope error of the grating is taken to be ±0.1 arcsec and both slits are set at 10 μm.

With the help of the *SHADOW* ray-tracing programs (Lai & Cerrina, 1986), the calcuated photon fluxes for different gratings

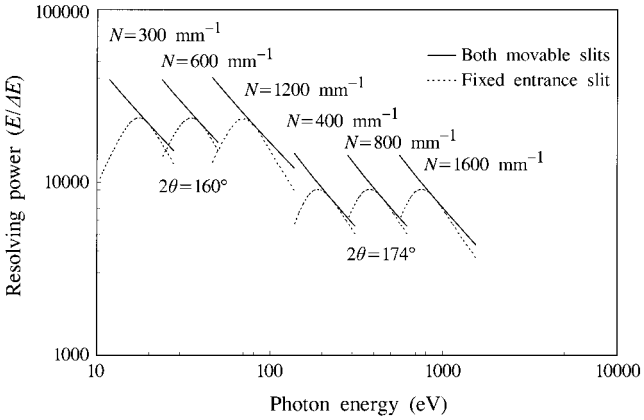

Figure 2
Calculated resolving power of the wide-range 6 m-SGM beamline. The dashed curves are with a fixed entrance slit and a movable exit slit, while the solid curves are with both slits movable to meet the Rowland-circle conditions. In these calculations, both slits are set at 10 μm.

and slit openings are shown in Fig. 3. In these calculations, the reflectance of all the optical surfaces, mirrors and gratings, are calculated using the Fresnel equations and the tabulated refraction coefficients, n and k (Mahan, 1956; Windt *et al.*, 1988). With a storage-ring current of 200 mA, a photon flux of 1×10^{11} photons s^{-1} is expected for an energy-resolving power of 20 000.

4. Summary

A high-performance wide-range 6 m-SGM beamline which covers photon energies from 10 to 1500 eV has been designed and is under construction at SRRC. Based on the 6 m-SGM design, several special features, such as specially designed bendable horizontal focusing mirrors, movable entrance slits, a bendable vertical focusing mirror and a movable exit slit, have been adopted to enhance the beamline performance greatly. Two or more end-stations can be installed in the beamline at the same time, allowing the beam time to be utilized fully. The expected photon flux is greater than 1×10^{11} photons s^{-1} for an energy-resolving power of 20 000. The size of the focused spot at the sample location is less than 0.7×0.3 mm^2. The beamline will be ready for commissioning in the spring of 1998.

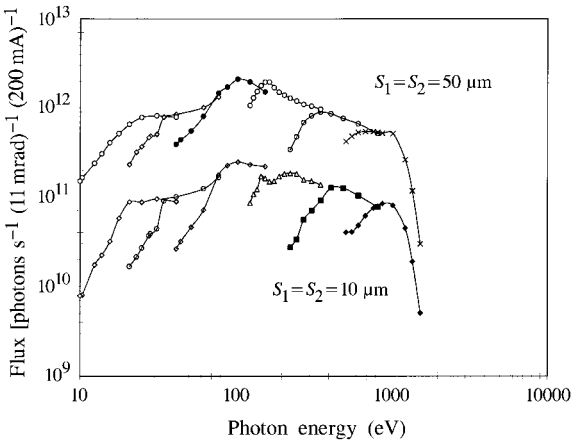

Figure 3
Calculated photon flux of the wide-range 6 m-SGM beamline. Flux curves for two different slit openings are shown.

We would like to thank the SRRC staff, especially the beamline group, for useful discussions.

References

Chen, C. T. (1987). *Nucl. Instrum. Methods A*, **256**, 595–604.
Chen, C. T. & Sette, F. (1989). *Rev. Sci. Instrum.* **60**, 1616–1621.
Chen, C. T. (1997). In preparation.
Chung, S.-C., Chen, C.-I., Tseng, P.-C., Lin, H.-F., Dann, T.-E., Song, Y.-F., Hsieh, T.-F., Tsang, K.-L. & Chang, C.-N. (1995). *Rev. Sci. Instrum.* **66**, 1655–1657.
Domke, M., Mandel, T., Puschman, A., Xue, C., Shirley, D. A. & Kanindl, G. (1992). *Rev. Sci. Instrum.* **63**, 80–89.
Jark, W. (1992). *Rev. Sci. Instrum.* **63**, 1241–1246.
Kanindl, G., Domke, M., Lambschat, C., Weschke, E. & Xue, C. (1992). *Rev. Sci. Instrum.* **63**, 1234–1240.
Koike, M. & Namioka, T. (1994). *Appl. Opt.* **33**, 2048–2056.
Koike, M. & Namioka, T. (1995). *Rev. Sci. Instrum.* **66**, 2144–2146.
Lai, B. & Cerrina, F. (1986). *Nucl. Instrum. Methods A*, **246**, 337–341.
Mahan, A. I. (1956). *J. Opt. Soc. Am.* **46**, 913–926.
Petersen, H. (1982). *Opt. Commun.* **40**, 402–406.
Samson, J. A. (1967). *Techniques of VUV Spectroscopy*, pp. 43–84. Nebraska, USA.
Schulz, K., Kanindl, G., Domke, M., Bozek, J. D., Heimann, P.A., Schlachter, A. S. & Rost, J. M. (1996). *Phys. Rev. Lett.* **77**, 3086–3089.
Tseng, P.-C., Lin, H.-J., Chung, S.-C., Chen, C.-I., Lin, H.-F., Dann, T.-E., Song, Y.-F., Hsieh, T.-F., Tsang, K.-L. & Chang, C.-N. (1995). *Rev. Sci. Instrum.* **66**, 1658–1660.
Warwick, T., Heimann, P., Mossessian, D., McKinney, W. & Padmore, H. (1995). *Rev. Sci. Instrum.* **66**, 2037–2040.
Windt, D. L., Cash, W. C., Scoot, M., Arendt, P., Newnam, B., Fisfer, R. F., Swartzlander, S., Takacs, P. Z. & Pinneo, J. M. (1988). *Appl. Opt.* **27**, 279–295.